INTERNATIONAL JOURNAL FOR NUMERICAL METHODS IN FLUIDS, VOL. 24, 319–336 (1997)

COUPLING BETWEEN LAMINAR FILM CONDENSATION AND NATURAL CONVECTION ON OPPOSITE SIDES OF A VERTICAL PLATE

HAN-TAW CHEN AND SHIUH-MING CHANG

Department of Mechanical Engineering, National Cheng Kung University, Tainan 701, Taiwan

SUMMARY

Theoretical analyses which incorporate one-dimensional heat conduction along a plate and transverse heat conduction approximations are presented to predict the net heat transfer between laminar film condensation of a saturated vapour on one side of a vertical plate and boundary layer natural convection on the other side. It is assumed that countercurrent boundary layer flows are formed on the two sides. The governing boundary layer equations of this problem and their corresponding boundary conditions are all cast into dimensionless forms by using a non-similarity transformation. Thus the resulting system of equations can be solved by using the local non-similarity method for the boundary layer equations and a finite difference method for the heat conduction equation of the plate. The plate temperature and the heat flux through the plate are repetitively determined until the solutions for each side of the plate match. The predicted results show that the effect of Pr_c is not negligible for larger values of A^* (thermal resistance ratio between natural convection side and condensing film side) and the approximation of transverse heat conduction overpredicts the plate temperature for lower values of R_t (thermal resistance ratio between plate and condensing film). However, no significant differences are observed between the two different approximations for higher values of R_t.

KEY WORDS: coupling; film condensation; natural convection

INTRODUCTION

Heat transfer across a vertical wall separating two semi-infinite fluid reservoirs at different temperatures has practical importance in numerous thermal engineering applications, such as nuclear reactor cooling, heat exchangers, thermal insulation of buildings, etc. The thermal interaction involved is for the most part inherent in the design of the heat transfer apparatus. Owing to its importance, various methods have been proposed to analyse such problems.[1–10] Faghri and Sparrow[7] studied the conjugate problem of thin film condensation on the outside of a vertical pipe and fully developed forced convection of a cold fluid inside the pipe. Poulikakos[8] presented a theoretical analysis for examining the phenomenon of conjugate laminar film condensation of a saturated vapour on one side of a vertical wall and laminar natural convection on the other side. In that work the natural convection Prandtl number Pr_c is assumed to approach infinity. Owing to this assumption, inertia terms in the momentum equation can be neglected compared with viscous and buoyancy terms. Furthermore, the Oseen linearization method[9] and the Nusselt–Rohsenow model were employed to simplify the natural convection and condensation problems respectively. However, the effect of the plate thermal resistance on the interaction between the two different heat transfer systems was not taken into account in this earlier work. Numerical results given by Poulikakos

CCC 0271–2091/97/030319–18

Received November 1994
Revised January 1996

showed that omitting the inertia terms of the momentum equation on the natural convection side can yield acceptable results (accurate to within 10%) even for $Pr_c = O(1)$. On the other hand, the overall heat transfer rate can be regarded as a weak function of Pr_c. Moreover, it was found in Reference 8 that the step size of the plate temperature T_w must be very small to obtain accurate results.

The present study proposes a mathematical model to investigate the conjugate problem of laminar film condensation and laminar natural convection separated by a vertical plate. It was shown in Reference 10 that the plate temperature distribution can be approximately determined by using a one-dimensional heat conduction equation provided that the aspect ratio (thickness/height) t/L is sufficiently small. The main purpose of the current study is to investigate the difference between the present results using a one-dimensional model of heat conduction along the plate and transverse heat conduction and those given by Poulikakos[8] for various important parameters, such as the thermal resistance of natural convection to film, A^*, the natural convection Prandtl number Pr_c and the thermal resistance of plate to film, R_t. Furthermore, the effect of A^*, Pr_c and R_t on the thermal interaction through the plate between the two different systems will also be discussed. It should be noted that both the plate temperature and the heat flux through the plate are unknown *a priori* in the present problem. Thus the boundary layer equations on both sides of the plate and the one-dimensional heat conduction equation for the vertical plate must be solved simultaneously. This was accomplished by using the two-equation model of the local non-similarity method[11] in conjunction with the Nachtsheim–Swigert iteraction scheme[12] and a finite difference approximation.

MATHEMATICAL FORMULATION

The physical geometry of this study and the co-ordinate system are shown in Figure 1, where a vertical impermeable plate of height L and thickness t separates two semi-infinite fluid reservoirs at different temperatures. The warmer reservoir, at a uniform temperature T_{sat}, contains a saturated vapour. The ambient temperature on the natural convection side is T_c. Owing to gravity, a continuous laminar film of condensate occurs on the condensatin side of the plate and flows downwards along the plate. It should be noted that liquid and vapour boundary layers exist simultaneously on the condensation side. The heating effect of the condensation side can give rise to an upward flow along the plate on the natural convection side. Thus the two fluid streams move in opposite directions for this problem. This analysis is restricted to the case where steady state conditions have been reached and the flows are laminar. It is also assumed that the physical properties of the natural convection are constant, except for the density in the buoyancy term, and the assumptions for film condensation

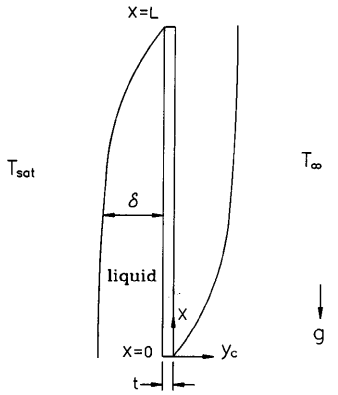

Figure 1. Physical geometry of system

along a vertical plate proposed by Koh *et al.*[13] are employed in the present study. Based on these assumptions, this problem can be formulated in terms of the boundary layer equations for the two different fluid streams and the one-dimensional heat conduction equation for the plate. It will be shown that these governing differential equations can be considered separately. Thermal coupling is achieved by the governing heat conduction equation for the vertical plate separating the two heat transfer systems.

Natural convection side

The dimensionless forms of the boundary layer equations expressing the conservation of mass, momentum and energy for the natural convection system shown in Figure 1 can be written as

$$\frac{\partial u_c}{\partial \xi_c} + \frac{\partial v_c}{\partial y_c^*} = 0, \tag{1}$$

$$\frac{1}{Pr_c}\left(u_c \frac{\partial u_c}{\partial \xi_c} + v_c \frac{\partial u_c}{\partial y_c^*}\right) = \theta_c + 0{\cdot}5 + \frac{\partial^2 u_c}{\partial y_c^{*2}}, \tag{2}$$

$$u_c \frac{\partial \theta_c}{\partial \xi_c} + v_c \frac{\partial \theta_c}{\partial y_c^*} = \frac{\partial^2 \theta_c}{\partial y_c^{*2}}, \tag{3}$$

with boundary conditions

$$u_c = v_c = 0 \quad \text{and} \quad \theta_c = \theta_r^*(\xi) \quad \text{at } y_c^* = 0, \tag{4a}$$

$$u_c = 0 \quad \text{and} \quad \theta_c = -0{\cdot}5 \quad \text{as } y_c^* \to \infty. \tag{4b}$$

The dimensionless parameters in equations (1)–(4) are defined as

$$y_c^* = Ra_c^{1/4} y_c/L, \qquad \xi_c = x/L, \qquad Pr_c = \nu_c/\alpha_c, \qquad u_c = \tilde{u}_c L/\alpha_c Ra_c^{1/2}, \; v_c = \tilde{v}_c L/\alpha_c Ra_c^{1/4},$$
$$\theta_c = [T_c - (T_{sat} + T_\infty)/2]/(T_{sat} - T_\infty)T_{sat} - T_\infty), \tag{5}$$

where Ra_c is the natural convection Rayleigh number and is defined as $Ra_c = g\beta(T_{sat} - T_\infty)L^3/\nu_c\alpha_c$. T_∞ denotes the freestream temperature in the natural convection system. $\theta_r^*(\xi)$ denotes the dimensionless plate temperature facing the natural convection side, $\theta_{wc}(\xi)$, when the approximation of transverse heat conduction is considered. However, $\theta_r^*(\xi)$ denotes the dimensionless plate temperature $\theta_w(\xi)$ for the case using the approximation of one-dimensional heat conduction along the plate. θ_{wc} and θ_w are defined as $\theta_{wc} = [T_{wc} - (T_{sat} + T_\infty)/2]/(T_{sat} - T_\infty)$ and $\theta_w = [T_w - (T_{sat} + T_\infty)/2]/(T_{sat} - T_\infty)$. The boundary condition $\theta_c = \theta_{wc}(\xi_c)$ at $y_c^* = 0$ will be assumed when heat conduction along the vertical plate is negligible. However, the boundary condition at $y_c^* = 0$ is $\theta_c = \theta_w(\xi_c)$ when the approximation of one-dimensional heat conduction along the plate is considered.

Film condensation side

The dimensionless boundary layer equations expressing the conservation of mass, momentum and energy for the condensation system can be written as follows.

Liquid

$$\frac{\partial u_s}{\partial \xi} + \frac{\partial v_s}{\partial y_s^*} = 0, \tag{6}$$

$$Jp_s\left(u_s \frac{\partial u_s}{\partial \xi} + v_s \frac{\partial u_s}{\partial y_s^*}\right) = 1 + \frac{\partial^2 u_s}{\partial y_s^{*2}}, \tag{7}$$

$$Ja_s\left(u_s \frac{\partial \theta_s}{\partial \xi} + v_s \frac{\partial \theta_s}{\partial y_s^*}\right) = \frac{\partial^2 \theta_s}{\partial y_s^{*2}}. \tag{8}$$

The dimensionless parameters in equations (6)–(8) are given as

$$\begin{aligned} &y_s^* = Ra_s^{1/4} y_s/L, \qquad \xi = 1 - \xi_c, \qquad u_s = \tilde{u}_s \mu_s Ra_s^{1/2}/g(\rho_s - \rho_v)L^2, \\ &v_s = \tilde{v}_s \mu_s Ra_s^{3/4}/g(\rho_s - \rho_v)L^2, \qquad \theta_s = [T_s - (T_{sat} + T_\infty)/2/(T_{sat} - T\infty), \end{aligned} \tag{9}$$

where Ja_s is the film Jakob number, Pr_s is the film Prandtl number, Jp_s is the ratio of Ja_s to Pr_s, and Ra_s is the film Rayleigh number. These dimensionless numbers are defined respectively as

$$\begin{aligned} &Ja_s = c_{ps}(T_{sat} - T_\infty)/h_{fg}, \qquad Pr_s = \nu_s/\alpha_s, \qquad Jp_s = Ja_s/Pr_s, \\ &Ra_s = g(\rho_s - \rho_v)L^3 h_{fg}/k_s \nu_s (T_{sat} - T_\infty). \end{aligned} \tag{10}$$

Vapor

It is assumed that the pure vapor outside the condensate layer is at the saturation temperature. Thus only the continuity and momentum equations are required for the vapour phase:

$$\frac{\partial u_v}{\partial \xi} + \frac{\partial v_v}{\partial y_v^*} = 0, \tag{11}$$

$$Jp_v\left(u_v \frac{\partial u_v}{\partial \xi} + v_v \frac{\partial u_v}{\partial y_v^*}\right) = \frac{\partial^2 u_v}{\partial y_v^{*2}}. \tag{12}$$

The dimensionless parameters in equations (11) and (12) are defined as

$$\begin{aligned} &y_v^* = Ra_v^{1/4}(y_s - \delta)/L, \qquad u_v = \tilde{u}_v \mu_v Ra_v^{1/2}/g(\rho_s - \rho_v)L^2, \qquad v_v = \tilde{v}_v \mu_v Ra_v^{3/4}/g(\rho_s - \rho_v)L^2, \\ &Ja_v = c_{p_v}(T_{sat} - T_\infty)/h_{fg}, \qquad Pr_v = \nu_v/\alpha_v, \qquad Jp_v = Ja_v/Pr_v, \\ &Ra_v = g(\rho_s - \rho_v)L^3 h_{fg}/k_v \nu_v (T_{sat} - T_\infty), \end{aligned} \tag{13}$$

where Ja_v is the vapour Jakob number, Pr_v is the vapour Prandtl number, Jp_v is the ratio of Ja_v to Pr_v, and Ra_v is the vapour Rayleigh number.

The boundary conditions for the condensation system are

$$u_s = v_s = 0 \quad \text{and} \quad \theta_s = \theta_1^*(\xi) \quad \text{at } y_s^* = 0, \tag{14a}$$

$$u_v \to 0 \quad \text{as } y_v^* \to \infty, \tag{14b}$$

where $\theta_1^*(\xi)$ denotes the dimensionless plate temperature facing the condensation side, $\theta_{wh}(\xi)$, when the approximation of transverse heat conduction is considered. θ_{wh} is defined as $\theta_{wh} = [T_{wh} - (T_{sat} + T_\infty)/2]/(T_{sat} - T_\infty)$. $\theta_1^*(\xi)$ denotes $\theta_w(\xi)$ for the case in which one-dimensional heat conduction along the plate is considered.

Interface matching

The vapour velocity tangent to the liquid–vapour interface is the same as the liquid velocity when there is no slip. The vapour velocity approaches zero at some distance away from this interface. The compatibility requirements are that the velocity, mass transfer, shear force and temperature along the liquid–vapour interface must be matched. The dimensionless forms of these compatibility requirements are

$$u_s = \frac{\mu_s}{\mu_v}\left(\frac{Ra_s}{Ra_v}\right)^{1/2} u_v, \tag{15a}$$

$$u_s \frac{d\delta^*}{d\xi} - v_s = \frac{v_s}{v_v}\left(\frac{Ra_s}{Ra_v}\right)^{3/4}\left(u_v \frac{d\delta_v^*}{d\xi} - v_v\right), \tag{15b}$$

$$\frac{\partial u_s}{\partial y_s^*} = \left(\frac{Ra_s}{Ra_v}\right)^{1/4} \frac{\partial u_v}{\partial y_v^*}, \tag{15c}$$

$$\theta_s = 0{\cdot}5 \quad \text{at } y_s^* = \delta^*. \tag{15d}$$

The energy balance equation at the liquid–vapour interface is given as

$$\frac{\partial \theta_s}{\partial y_s^*} = \left(u_s \frac{d\delta^*}{d\xi} - v_s\right)[1 + B(0{\cdot}5 - \theta_1^*)] \quad \text{at } y_s^* = \delta^*, \tag{16}$$

where $B = \frac{3}{8} Ja_s$.

The dimensionless film thickness of the condensate, δ^*, is not known *a priori* and is one of the results of the present study, where $\delta^* = \delta Ra_s^{1/4}/L$. The value of δ^* can be obtained from equation (16).

Vertical plate

(a) Assume that the effect of heat conduction along the plate is negligible in comparison with transverse heat conduction. Under this condition the heat flux entering the left face of the plate must be equal to that leaving the right face at any given vertical position. Thus the dimensionless form of this condition can be written as

$$-\left.\frac{\partial \theta_c}{\partial y_c^*}\right|_{y_c^*=0} = A^* \left.\frac{\partial \theta_s}{\partial y_s^*}\right|_{y_s^*=0} = \frac{\theta_{wh} - \theta_{wc}}{R_t^*}, \tag{17}$$

where A^* can be regarded as the thermal resistance ratio of natural convection to film and is defined as $A^* = (k_s/k_c)(Ra_s/Ra_c)^{1/4}$, and R_t^* can be regarded as the thermal resistance ratio of plate to natural convection and is defined as $R_t^* = (k_c/k_w)(t/L)Ra_c^{1/4}$.

A correlation between θ_{wh} and θ_{wc} can be obtained from equation (17) as

$$\theta_{wc} = \theta_{wh} - R_t \left.\frac{\partial \theta_s}{\partial y_s^*}\right|_{y_{s=0}^*}, \tag{18}$$

where R_t can be regarded as the thermal resistance ratio of plate to film and is defined as $R_t = (k_s/k_w)(t/L)Ra_s^{1/4}$. The limiting case of $R_t = 0$ corresponds to the plate having no thermal resistance between the two different heat transfer systems. This implies that θ_{wc} is equal to θ_{wh} for $R_t = 0$.

(b) Assume that the aspect ratio t/L is sufficiently small. Under this circumstance the variation in the plate temperature can be obtained approximately from the following one-dimensional heat conduction equation along the plate:

$$\frac{\mathrm{d}^2\theta_w}{\mathrm{d}\xi^2} - \frac{h_{xc}(\theta_w + 0{\cdot}5)L^2}{k_w t} - \frac{h_{xs}(\theta_w - 0{\cdot}5)L^2}{k_w t} = 0, \tag{19}$$

where h_{xs} and h_{xc} are the local heat transfer coefficients for the film and natural convectin systems respectively. The coefficients h_{xs} and h_{xc} to be used in equation (19) are the outcome of the solutions of the boundary layer equations, while the thermal boundary conditions corresponding to the boundary layer equations are the outcome of the solutions of the one-dimensional heat conduction equation.

The thermal bounday conditions at $y_s^* = 0$ and $y_c^* = 0$ corresponding to the boundary layer equations can be written as

$$k_s Ra_s^{1/4} \left.\frac{\partial\theta_s}{\partial y_s^*}\right|_{y_{s=0}^*} = Lh_{xs}(0{\cdot}5 - \theta_w), \tag{20}$$

$$-k_c Ra_c^{1/4} \left.\frac{\partial\theta_c}{\partial y_c^*}\right|_{y_{c=0}^*} = Lh_{xc}(0{\cdot}5 + \theta_w). \tag{21}$$

Substituting equations (20) and (21) into equation (19) yields

$$\frac{\mathrm{d}^2\theta_w}{\mathrm{d}\xi^2} + A^* R_t^* \left.\frac{\partial\theta_s}{\partial y_s^*}\right|_{y_{s=0}^*} + R_t^* \left.\frac{\partial\theta_c}{\partial y_c^*}\right|_{y_{c=0}^*} = 0. \tag{22}$$

The corresponding boundary conditions are

$$\frac{\mathrm{d}\theta_w}{\mathrm{d}\xi} = 0 \quad \text{at } \xi = 0 \text{ and } 1. \tag{23}$$

To compare the present results with those given by Poulikakos,[8] the Nusselt–Rohsenow model for the condensation problem is introduced into the present analysis, so that equations (7) and (8) can be simplified as

$$1 + \frac{\partial^2 u_s}{\partial y_s^{*2}} = 0, \tag{24}$$

$$\frac{\partial^2\theta_s}{\partial y_s^{*2}} = 0. \tag{25}$$

The two-equation model of the local non-similarity method[11] is applied to solve equations (1)–(3), (6)–(8), (11) and (12) together with boundary conditions (4) and (14)–(16). Thus the similarity variables η_c, η_s and η_v and the reduced streamfunctions f_c, f and F are defined as

$$\eta_c = y_c^*/\xi_c^{1/4}, \qquad \psi_c = \xi_c^{3/4} f_c(\xi_c, \eta_c), \tag{26a}$$

$$\eta_s = y_s^*/\xi^{1/4}, \qquad \psi_s = \xi^{3/4} f(\xi, \eta_s), \tag{26b}$$

$$\eta_v = y_v^*/\xi^{1/4}, \qquad \psi_v = \xi^{3/4} F(\xi, \eta_v), \tag{26c}$$

where ψ_c, ψ_s and ψ_v denote the streamfunctions and are defined by $u_c = \partial\psi_c/\partial y_c^*$, $v_c = -\partial\psi_c/\partial\xi_c$, $u_s = \partial\psi_s/\partial y_s^*$, $v_s = -\partial\psi_s/\partial\xi$, $u_v = \partial\psi_v/\partial y_v^*$ and $v_v = -\partial\psi_v/\partial\xi$. It is evident that these definitions satisfy the continuity equations (1), (6) and (11).

Owing to the introduction of the dimensionless parameters defined in equations (5), (9) and (26), the partial differential equations (2), (3), (24) and (25) can be transformed into the ordinary differential equations

$$f_c''' + (3f_c f_c''/4 - f_c'^2/2)/Pr_c + \theta_c + 0{\cdot}5 = \xi_c(f_c' g_c' - f_c'' g_c)/Pr_c, \tag{27}$$

$$\theta_c'' + 3f_c\theta_c'/4 = \xi_c(f_c'\varphi_c - \theta_c' g_c), \tag{28}$$

$$f''' + 1 = 0, \tag{29}$$

$$\theta_s'' = 0, \tag{30}$$

where $g_c = \partial f_c/\partial\xi_c$ and $\varphi_c = \partial\theta_c/\partial\xi_c$. The primes denote differentiation with respect to η_c for the natural convection system and with respect to η_s for the film layer.

Two additional differential equations can be obtained by differentiating equations (27) and (28) with respect to ξ_c. To close the system of boundary layer equations at the second-order level, terms involving $\partial g_c/\partial\xi_c$ and $\partial\varphi_c/\partial\xi_c$ in the resulting equations are ignored. Thus the two additional differential equations are expressed as

$$g_c''' + (3f_c g_c''/4 + 7g_c f_c''/4 - 3f_c' g_c')/Pr_c + \varphi_c = \xi_c(g_c'^2 - g_c'' g_c)/Pr_c, \tag{31}$$

$$\varphi_c'' + 3f_c'\varphi_c'/4 + 7g_c\theta_c'/4 - f_c'\varphi_c = \xi_c(g_c'\varphi_c - \varphi_c' g_c). \tag{32}$$

It is evident that equations (27)–(32) constitute a set of ordinary differential equations. The complete set of boundary conditions is given as

$$f_c = f_c' = g_c = g_c' = 0 \quad \text{and} \quad \theta_c = \theta_r^* \quad \text{at } \eta^c = 0, \tag{33a}$$

$$f_c' = g_c' = 0, \theta_c = -0{\cdot}5 \quad \text{and} \quad \varphi_c = 0 \quad \text{as } \eta_c \to \infty, \tag{33b}$$

$$f = f' = 0 \quad \text{and} \quad \theta_s = \theta_1^*(\xi) \quad \text{at } \eta_s = 0, \tag{34a}$$

$$f'' = 0 \quad \text{and} \quad \theta_s = 0{\cdot}5 \quad \text{at } \eta_s = \eta_{si}, \tag{34b}$$

$$1 = [1 + B(0{\cdot}5 - \theta_1^*)][3f/(4\theta_s')]_{\eta_s=\eta_{si}}, \tag{z34c}$$

where $\eta_{si} = Ra_s^{1/4}\delta/L\xi^{1/4}$.

The solutions of equations (29) and (30) which satisfy boundary conditions (34a) and (34b) are

$$f = -\eta_s^3/6 + \eta_{si}\eta_s^2/2, \tag{35}$$

$$\theta_s = [0{\cdot}5 - \theta_1^*(\xi)]\eta_s/\eta_{si} + \theta_1^*(\xi). \tag{36}$$

Substituting equations (35) and (36) into equations (34c) yields

$$\theta_1^*(\xi) = 0{\cdot}5 - \eta_{si}^4/(4 - B\eta_{si}^4). \tag{37}$$

It can be seen that the dimensionless plate temperature θ_1^* can be determined from equation (37) provided that the value of η_{si} is given.

Substitution of equation (26) into equations (17) and (22) yields the following requirements at the plate:

$$\theta_c'(1-\xi,0) = -A^*[(1-\xi)/\xi]^{1/4}\theta_s'(\xi,0), \tag{38}$$

$$\frac{d^2\theta_w}{d\xi^2} + A^*R_t^*\xi^{-1/4}\theta_s'(\xi,0) + R_t^*(1-\xi)^{-1/4}\theta_c'(1-\xi,0) = 0. \tag{39}$$

The differential form of equation (39) can be written as

$$\frac{\theta_{w,p-1} - 2\theta_{w,p} + \theta_{w,p+1}}{\Delta\xi^2} + R_t^*A^*\xi_p^{-1/4}\theta_s'(\xi_p,0) + R_t^*(1-\xi_p)^{-1/4}\theta_c'(1-\xi_p,0) = 0 \quad \text{for } p = 1,2,\ldots,N, \tag{40}$$

where $\xi_1 = 0$, $\xi_N = L$, $\Delta\xi = \xi_{p+1} - \xi_p$ and N denotes the total nodal number for the vertical plate.

The local heat transfer coefficient h_{xc} for the natural convection system can be expressed as

$$h_{xc} = -k_c \left.\frac{\partial T_c}{\partial y_c}\right|_{y_c=0} \Big/ [T_c(x, y_c = 0) - T_\infty] = -q_{xc}/[T_c(x, y_c = 0) - T_\infty], \tag{41}$$

where q_{xc} denotes the local heat flux through the right face of the vertical plate and is defined as $q_{xc} = -k_c(\partial T_c/\partial y_c)|y_c = 0$. Furthermore, the local Nusselt number Nu_{xc} for the natural convection system can be obtained from the substitution of the dimensionless variables in equations (5) and (26a) into equation (41):

$$Nu_{xc} = h_{xc}x/k_c = -Ra_c^{1/4}\xi_c^{3/4}\theta_c'(\xi_c,0)/(\theta_r^* + 0{\cdot}5). \tag{42}$$

The total heat flux Q through the right face of the vertical plate is obtained by numerically integrating q_{xc} over the entire height of the plate, i.e.

$$Q = -k_c \int_0^L \left(\left.\frac{\partial T_c}{\partial y_c}\right|_{y_c=0} \right) dx. \tag{43}$$

The value of Q can be numerically obtained by using the trapezoidal rule. Substituting equations (5) and (26a) into equation (43) gives the dimensionless form of Q as

$$\tilde{Q} = \frac{Q}{k_c(T_{sat} - T_\infty)} = -Ra_c^{1/4} \int_0^1 [\theta_c'(\xi_c, \eta_c = 0)/\xi_c^{1/4}] d\xi_c = SRa_c^{1/4}, \tag{44}$$

where $S = -\int_0^1 [\theta_c'(\xi_c, \eta_c = 0)/\xi_c^{1/4}] d\xi_c$.

The average heat transfer coefficient $\bar{h}_c$ for a height L can be defined as

$$\bar{h}_c = \frac{1}{L(T_{sat} - T_\infty)} \int_0^L q_{xc} dx. \tag{45}$$

Accordingly, the average Nusselt number Nu_c can be derived as

$$Nu_c = \bar{h}_c L/k_c = \tilde{Q}. \tag{46}$$

Solution procedures

The computational procedures for solving this problem are listed in the following.

1. First a value of η_{si} at $\xi = \Delta\xi$ is guessed. Accordingly, the boundary layer equations (27), (28), (31) and (32) together with the boundary conditions (33a) an d(33b) can be solved by using the fourth-order Runge–Kutta method in conjunction with the Nachtsheim–Swigert iteration

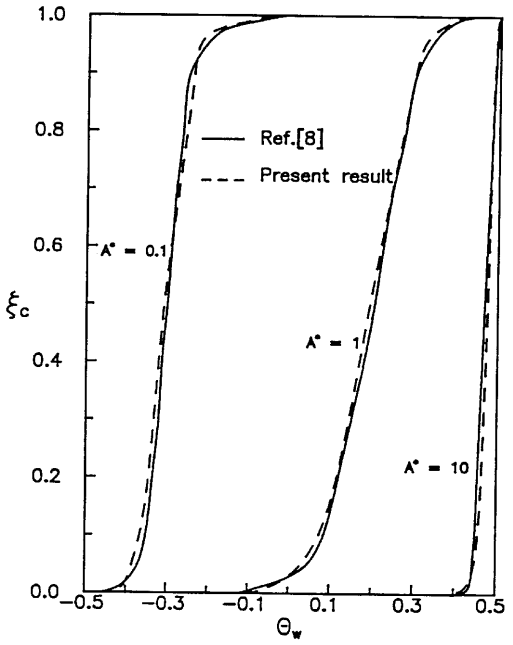

Figure 2. Comparison of θ_w for $Pr_c \to \infty, R_t = 0, B = 1$ and various A*-values

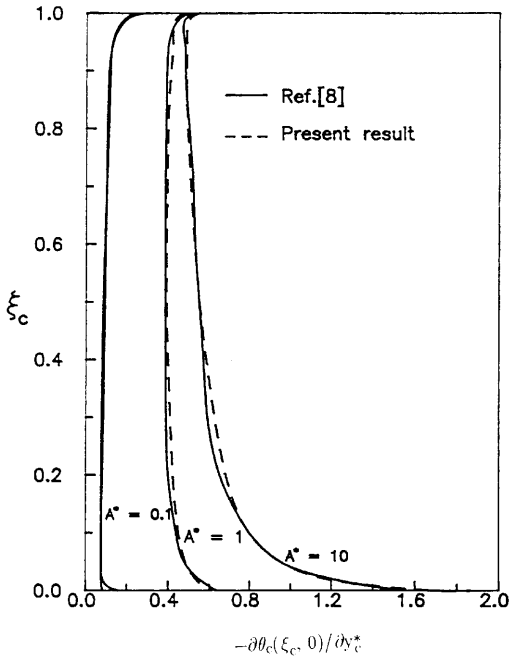

Figure 3. Comparison of $-\partial\theta_c(\xi_c, 0)/\partial y_c^*$ for $Pr_c \to \infty, R_t = 0, B = 1$ and various A*-values

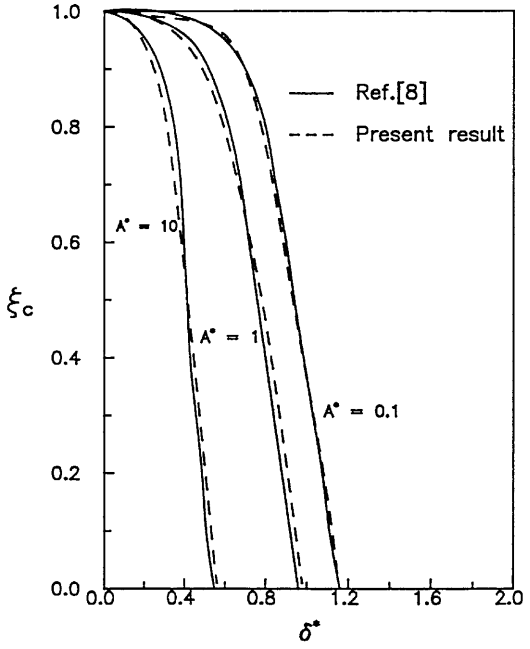

Figure 4. Comparison of δ^* for $Pr_c = \infty$, $R_t = 0$, $B = 1$ and various A^*-values

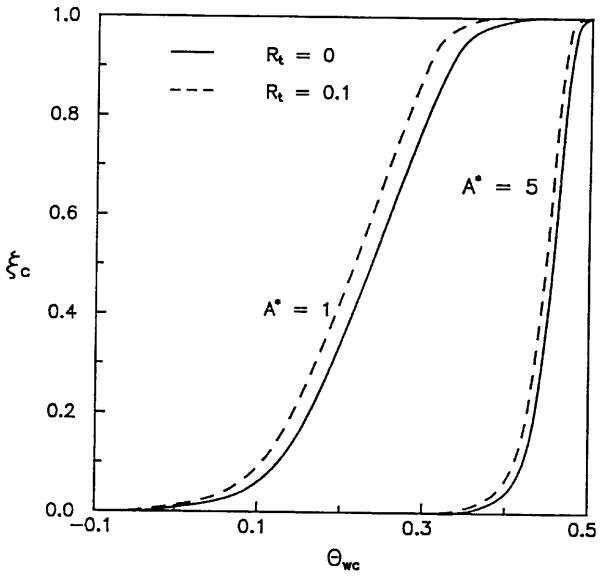

Figure 5. Effect of A^* on θ_{wc} for $B = 1$, $Pr_c = 0{\cdot}7$ and various R_t-values

scheme[12] for the natural convection system. Afterwards, equation (38) or equation (40) in conjunction with equations (36) and (37) is solved in order to determine the nodal plate temperature. The entire calculation is repeated until the requirements at the plate are satisfied. Otherwise a new guess for η_{si} will be given until all the convergent criteria are satisfied.

2. The computational processes of step 1 are repeated by advancing a small space step $\Delta\xi$ until $\xi = 1 - \Delta\xi$. (Note that the points at $\xi = 0$ and 1 are singular.)
3. The entire computational procedure is complete when the plate temperature distribution obtained from steps 1 and 2 does not change.

All computations are performed on a personal computer with an 80486 microprocessor. The present numerical results were obtained by using 51 nodes for the natural convection system and nine nodes in the ξ-direction for the case with the approximation of transverse heat conduction (or 25 nodes for the case with the approximation of one-dimensional heat conduction along the plate). The number of iterations required for each case was less than seven.

RESULTS AND DISCUSSION

The difference between the results obtained from the complete boundary layer equations and those using the Nusselt–Rohsenow model was found to be small for low *Ja*-values. Because of this, the results obtained from the complete boundarylayer equations will not be shown in this paper. It should be noted that the present results in Figures 2–8 were obtained by using the transverse heat conduction approximation. Figures 2–4 show comparisons of the dimensionless plate temperature, θ_w, the dimensionless temperature gradient facing the natural convection side, $-\partial\theta_c(\xi_c, 0)/\partial y_c^*$, and the dimensionless thickness δ^* respectively between the present results and those given by Poulikakos[8] for $R_t = 0, B = 1, Pr_c \to \infty$ and various A^*-values. It is seen that the present results are in good agreement with those given by Poulikakos.[8]

Figures 5 and 6 show the effects of A^* on θ_{wc} and $-\partial\theta_c(\xi_c, 0)/\partial y_c^*$ respectively for $Pr_c = 0{\cdot}7, B = 1$ and various R_t-values. It can be observed from the definition of A^* that an increase in A^* can be regarded as an increase in the natural convection thermal resistance. Thus decreasing A^* enhances the heat transfer from the condensation side to the natural convection side. In other words, increasing A^* makes θ_{wc} tend to the saturation temperature and leads to an increase in $-\partial\theta_c(\xi_c, 0)/\partial y_c^*$ as shown in Figures 5 and 6. Another important observation from Figures 5 and 6 is that the effect of R_t on θ_{wc} and $-\partial\theta_c(\xi, 0)/\partial y_c^*$ is not very significant for higher A^*-values.

The effects of the natural convection Prandtl number Pr_c on θ_w and $-\partial\theta_c(\xi_c, 0)/\partial y_c^*$ for $A^* = B = 1$ and $R_t = 0$ are shown in Figures 7 and 8 respectively. These two figures show that decreasing Pr_c makes the value of θ_w tend to 0·5 and leads to a decrease in $-\partial\theta_c(\xi_c, 0)/\partial y_c^*$. A more important observation is that the effects of Pr_c on θ_w and $-\partial\theta_c(\xi_c, 0)/\partial y_c^*$ are not negligible. The numerical results given in Table I were obtained by using the transverse heat conduction approximation for $B = 1, R_t = 0$ and various A^*-values. It can be seen that $Nu_c/Ra_c^{1/4}$ is indeed a weak function of Pr_c for low A^*-values. However, the increase in $Nu_c/Ra_c^{1/4}$ is about 22% for $A^* = 10$ as Pr_c increase from 0·7 to ∞. The above results further demonstrate that the effect of Pr_c is not negligible for higher A^*-values. Another observation is that the value of $Nu_c/Ra_c^{1/4}$ for $A^* = 0{\cdot}1$ and $Pr_c = 0{\cdot}7$ is about 82% lower than that for $A^* = 10$ and $Pr_c = 0{\cdot}7$. Obviously, the effect of A^* is more pronounced than that of Pr_c.

The other purpose of the present study is to present the variation in the total heat flux through the plate with $\tilde{A}, Pr_s, Pr_c$ and Ja_s. This task can be performed by using a relationship of $Nu_c/Ra_c^{1/4}$ and these parameters with a single general expression, where $\tilde{A} = A^*(Pr_c Jp_s)^{1/4}$. The empirical

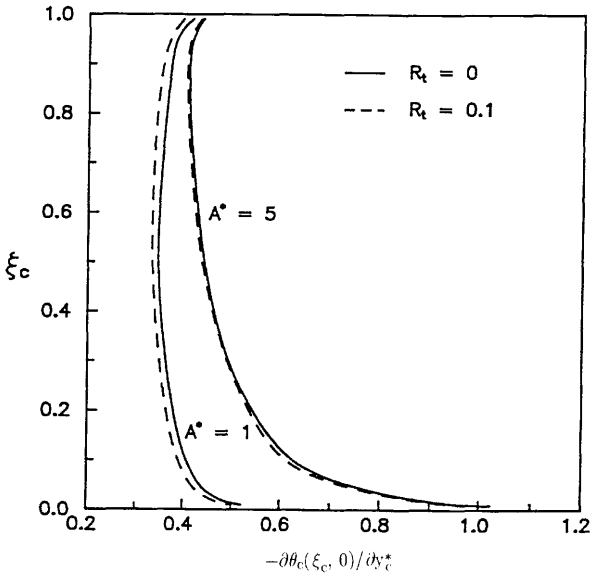

Figure 6. Effect of A^* on $-\partial\theta_c(\xi_c, 0)/\partial y_c^*$ for $B = 1$, $Pr_c = 0{\cdot}7$ and various R_t-values

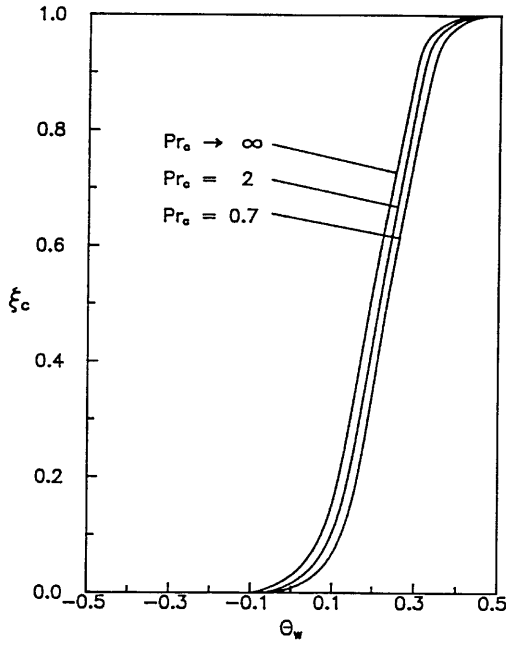

Figure 7. Effect of Pr_c on θ_w for $A^* = B = 1$ and $R_t = 0$

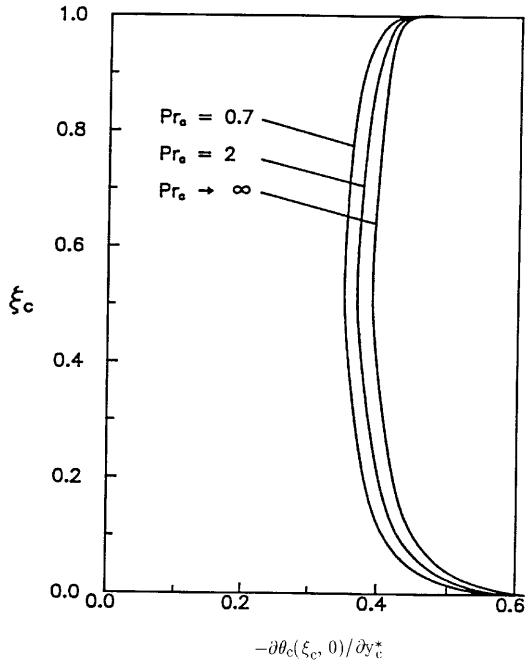

Figure 8. Effect of Pr_c on $-\partial\theta_c(\xi_c, 0)/\partial y_c^*$ for $A^* = B = 1$ and $R_t = 0$

correlation which presents all the computed values within 0·5% for $0{\cdot}1 \leqslant \tilde{A} \leqslant 1$, $1 \leqslant Pr_s \leqslant 3, 0{\cdot}7 \leqslant Pr_c \leqslant 10$ and $0{\cdot}01 \leqslant Ja_s \leqslant 0{\cdot}2$ is constructed. This correlation can be expressed as

$$\frac{Nu_c}{Ra_c^{0{\cdot}25}} = Pr_c^{-0{\cdot}25}\left[-1{\cdot}38665 + 5{\cdot}3485\left(\frac{\tilde{A}}{1+\tilde{A}}\right)^{0{\cdot}164} Ja_s^{-0{\cdot}0197} Pr_s^{0{\cdot}0305} \frac{Pr_c^{0{\cdot}209}}{(1+Pr_c^{0{\cdot}217})^{1{\cdot}11}}\right]. \tag{47}$$

The values of θ_{wc} and $-\partial\theta_c(\xi_c, 0)/\partial y_c^*$ predicted using the approximations of one-dimensional heat conduction along the plate and transverse heat conduction are presented in Figures 9 and 10 respectively for $A^* = 5, B = 1, L/t = 16, Pr_c = 0{\cdot}7$ and various R_t-values. It is seen that the θ_{wc}-value using the approximatin of one-dimensional heat conduction along the plate is lower than that using the approximation of transverse heat conduction for $R_t = 0{\cdot}1$. However, no obvious difference between them is found for $R_t = 1$. A similar result was described in Reference 10. Moreover, numerical results obtained by Viskanta and Lankford[3] also showed that the predicted plate

Table I. Variation in Pr_c with $Nu_c/Ra_c^{1/4}$ for $B = 1, R_t = 0$ and various A^*-values

	$Nu_c/Ra_c^{1/4}$		
Pr_c	$A^* = 10$	$A^* = 1$	$A^* = 0{\cdot}1$
0·7	0·5187	0·3828	0·0940
2	0·5684	0·4021	0·0942
∞	0·6322	0·4216	0·0944

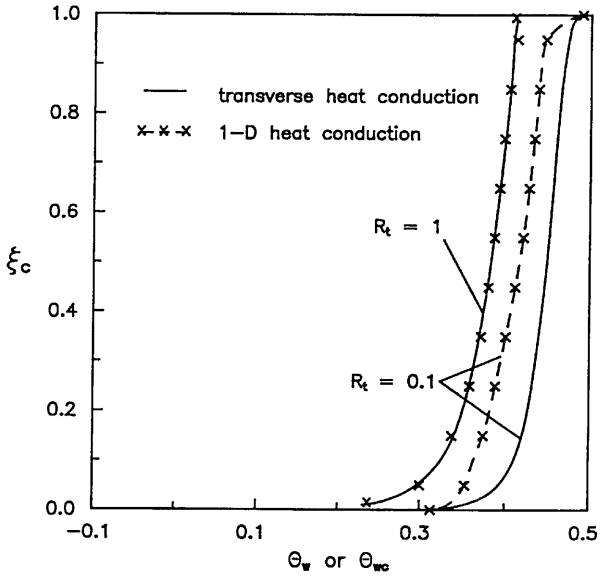

Figure 9. Comparison of plate temperature distribution for $Pr_c = 0{\cdot}7$, $A^* = 5$, $L/t = 16$, $B = 1$ and various R_t-values

temperature using the approximation of transverse heat conduction was higher than experimental values. This implies that it is difficult to obtain a more accurate result by using the transverse heat conduction approximation, especially for lower R_t-values. Based on the definition of R_t, a thicker wall means more effective insulation betwen the two reservoirs. Thus increasing R_t lowers the plate temperature on the side facing the natural convection and leads to an increase in the temperature difference across the plate. In other words, an increase in R_t leads to a reduction of $-\partial\theta_c(\xi_c, 0)/\partial y_c^*$

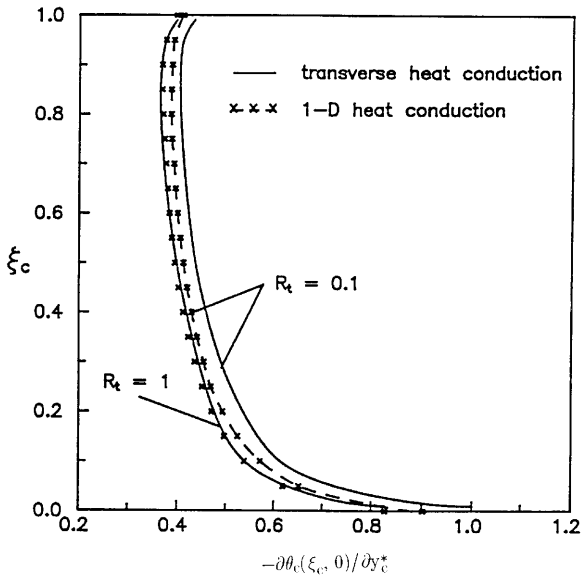

Figure 10. Comparison of $0 - \partial\theta_c(\xi_c, 0)/\partial y_c^*$ for $Pr_c = 0{\cdot}7$, $A^* = 5$, $L/t = 16$, $B = 1$ and various R_t-values

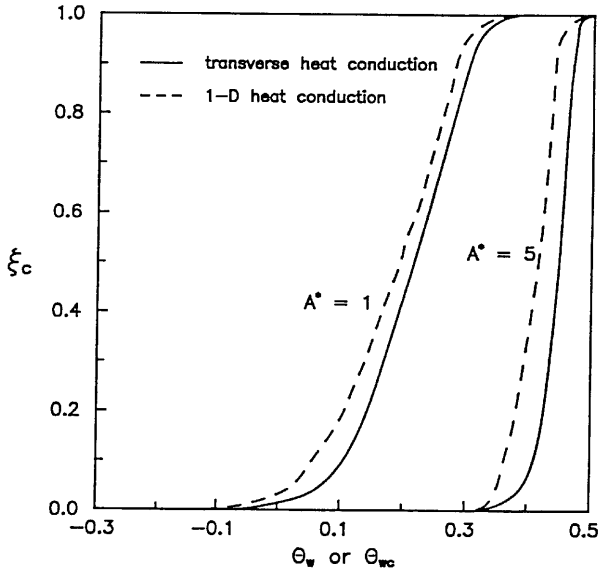

Figure 11. Comparison of plate temperature distribution for $Pr_c = 0{\cdot}7, R_t = 0{\cdot}1, L/t = 16, B = 1$ and various A*-values

and yields a more uniform plate temperature distribution that approaches the freestream temperature of the natural convection system. It can also be seen from Figure 10 that the areas under the curves of the dimensionless temperature gradient using the approximations of one-dimensional heat conduction along the plate and transverse heat conduction are almost identical for $R_t = 1$. However, the area using the approximation of transverse heat conduction is larger than that using the approximation of one-dimensional heat conduction along the plate for $R_t = 0{\cdot}1$.

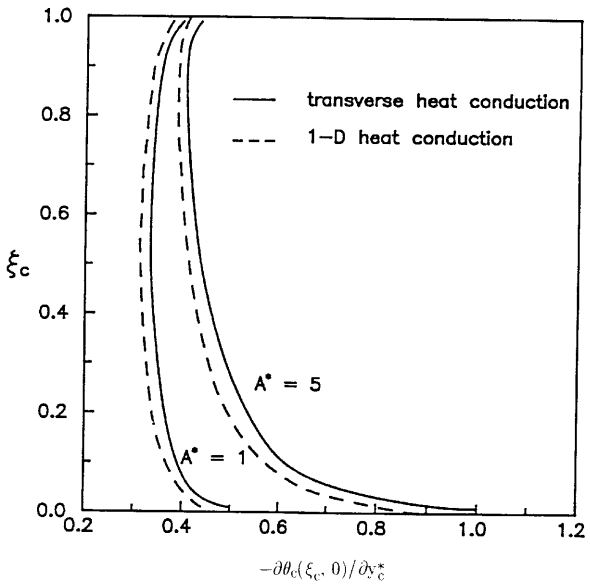

Figure 12. Comparison of $-\partial\theta_c(\xi_c, 0)/\partial y_c^*$ for $Pr_c = 0{\cdot}7, R_t = 0{\cdot}1, L/t = 16, B = 1$ and various A*-values

The results for θ_{wc} and $-\partial\theta_c(\xi_c, 0)/\partial y_c^*$ predicted the approximations of one-dimensional heat conduction along the plate and transverse heat conduciton for $B = 1, L/t = 16, Pr_c = 0{\cdot}7, R_t = 0{\cdot}1$ and various A^*-values are shown in Figures 11 and 12 respectively. It is clear that the values of θ_{wc} and $-\partial\theta_c(\xi_c, 0)/\partial y_c^*$ predicted using the approximation of transverse heat conduction are always higher than those predicted using the approximation of one-dimensional heat conduction along the plate for $R_t = 0{\cdot}1$ and $A^* = 1{\cdot}5$. Figure 12 also shows that the areas under the curves of the dimensionless temperature gradient $-\partial\theta_c(\xi_c, 0)/\partial y_c^*$ using the approximation of transverse heat conduction are larger than those using the approximation of one-dimensional heat conduction along the plate.

CONCLUSION

A numerical technique was used to investigate the conjugate problem of laminar film condensation and natural convection separated by a conducting vertical plate. Results show that the application of the Nusselt–Rohsenow model to describe the heat transfer phenomenon on the condensation side can give accurate predictions provided that Pr_s is of the order of unity or greater and Ja_s is less than unity. The major purpose of the present study was to investigate the difference in predicted results obtained by using the approximation of one-dimensional heat conduction along the plate and transverse heat conduction. It was found that the approximation of transverse heat conduction can overpredict the plate temperature and the overall heat transfer rate through the plate for lower R_t-values. However, no significant differences are observed between the two conduction models for higher R_t-values. Another important observation is that the effect of Pr_c is not negligible for higher A^*-values, while the effect of A^* seems to be more pronounced than that of other system parameters. The accuracy of the present results can only be evidenced through further experiments.

APPENDIX: NOMENCLATURE

A^*	thermal resistance of natural convection to film
$\tilde{A}$	dimensionless parameter, $A^*(Pr_c Jp_s)^{1/4}$
B	dimensionless parameter, $\frac{3}{8}\ Ja_s$
c_p	specific heat
f, f_c, F	reduced streamfunctions
g	gravitational acceleration
g_c	dimensionless function, $\partial f_c/\partial\xi_c$
h	heat transfer coefficient
h_x	local heat transfer coefficient
h_{fg}	latent heat of condensation
$\bar{h}_c$	average heat transfer coefficient for natural convection system
Ja	Jakob number
Jp	ratio of Ja to Pr
k	thermal conductivity
L	height of plate
N	total nodal number for plate
Nu_c	average Nusselt number defined in equation (46)
Nu_{xc}	local Nusselt number defined in equation (42)
Pr	Prandtl number
Q	total heat flux defined in equation (43)
$\tilde{Q}$	dimensionless total heat flux defined in equation (44)

Ra_c	natural convectin Rayleigh number, $g\beta(T_{sat} - T_\infty)L^3/\nu_c\alpha_c$
Ra_s	film Rayleigh number, $gL^3(\rho_s - \rho_v)h_{fg}/\nu_s k_s(T_{sat} - T_\infty)$
Ra_v	vapour Rayleigh number, $gL^3(\rho_s - \rho_v)h_{fg}/\nu_v k_v(T_{sat} - T_\infty)$
R_t^*	thermal resistance of plate to natural convection, $(k_c/k_w)(t/L)Ra_c^{1/4}$
S	integral value defined in equation (44)
t	thickness of plate
T	temperature
T_{sat}	saturation temperature
T_∞	freestream temperature
u, v	velocity components in x- and y-direction
$\tilde{u}, \tilde{v}$	dimensionless velocity components in x- and y-direction
x, y_c, y_s	co-ordinates
y_c^*, y_s^*	dimensionless co-ordinates

Greek letters

α	thermal diffusivity
β	coefficient of thermal expansion
δ	film thickness
δ^*	dimensionless film thickness
θ	dimensionless temperature, $[T - (T_{sat} + T_\infty)/2]/(T_{sat} - T_\infty)$
θ_1^*, θ_r^*	dimensionless plate temperature
μ	dynamic viscosity
ν	kinematic viscosity
ξ, ξ_c, η	dimensionless parameters
ξ_p	interior grid point in plate
ρ	density
φ_c	dimensionless function, $\partial\theta_c/\partial\xi_c$
ψ	streamfunction

Subscripts

c	in natural convection system
p	evaluation at $\xi = \xi_p$
s	in condensate film
si	at liquid–vapour interface
v	in vapour phase
w	at plate
wc	at right face of plate
wh	at left face of plate

REFERENCES

1. R. Viskanta and M. Abrams, 'Thermal interaction of two streams in boundary layer flow separated by a wall', *Int. J. Heat Mass Transfer*, **14**, 1311–1321 (1971).
2. G. S. H. Lock and R. S. Ko, 'Coupling through a wall between two free convective systems', *Int. J. Heat Mass Transfer*, **16**, 2087–2096 (1973).
3. R. Viskanta and D. W. Lankford, 'Coupling of heat transfer between two natural convection systems separated by a vertical wall', *Int. J. Heat Mass Transfer*, **24**, 1171–1177 (1981).

4. R. Anderson and A. Bejan, 'Natural convection on both sides of a vertical wall separating fluids at different temperatures', *ASME J. Heat Transfer*, **102**, 630–635 (1980).
5. A. Bejan and R. Anderson, 'Heat transfer across a vertical impermeable partition imbedded in porous medium'. *Int. J. Heat Transfer*, **24**, 1237–1245 (1981).
6. A. Bejan and R. Anderson, 'Natural convection at the interface between a vertical porous layer and an open space, *ASME J. Heat Transfer*, **105**, 124–129 (1983).
7. M. Faghri and E. M. Sparrow, 'Parallel flow and counterflow on an internally cooled vertical tube', *Int. J. Heat Mass Transfer*, **23**, 559–562 (1980).
8. D. Poulikakos, 'Interaction between film condensation on one side of a vertical wall and natural convection on the other side', *ASME J. Heat Transfer*, **108**, 560–566 (1986).
9. A. E. Gill, 'The boundary layer region for convection in a rectangular cavity', *J. Fluid Mech.*, **26**, 515–536 (1966).
10. H.-T. Chen and S.-M. Chang, 'Numerical simulation for conjugate problem of natural convection on both sides of a vertical wall', *Int. J. Heat Mass Transfer*, **39**, 383–390 (1996).
11. E. M. Sparrow and H. S. Yu, 'Local non-similarity thermal boundary-layer solution', *ASME J. Heat Transfer*, **93**, 328–336 (1971).
12. J. A. Adams and D. F. Rogers, *Computer-Aided Heat Transfer Analysis*, McGraw-Hill, New York, 1973.
13. J. C. Y. Koh, E. M. Sparrow and J. P. Hartnett, 'The two phase boundary layer in laminar film condensation', *Int. J. Heat Mass Transfer*, **2**, 69–82 (1961).